Entropy **2010**, *12*, 275-288; doi:10.3390/e12020275

OPEN ACCESS

entropy

ISSN 1099–4300

www.mdpi.com/journal/entropy

Article

Self-Organization during Friction in Complex Surface Engineered Tribosystems

German S. Fox-Rabinovich [1,*], Iosif S. Gershman [2], Kenji Yamamoto [3], Andrew Biksa [1], Stephen C. Veldhuis [1], Ben D. Beake [4] and Anatoliy I. Kovalev [5]

[1] Department of Mechanical Engineering, McMaster University, 1280 Main St., W. Hamilton, Ontario L8S 4L7, Canada

[2] Railway Transport Research Institute, Moscow 29851, Russia

[3] Kobe Steel Ltd., Kobe, Hyogo 651–2271, Japan

[4] Micro Materials Ltd., Wrexham LL13 7YP, UK

[5] Surface Phenomena Research Group, CNIICHERMET, Moscow 105005, Russia

* Author to whom correspondence should be addressed; E-Mail: gfox@mcmaster.ca.

Received: 15 October 2009; in revised form: 5 January 2010 / Accepted: 23 February 2010 / Published: 25 February 2010

Abstract: Self-organization during friction in complex surface engineered tribosystems is investigated. The probability of self-organization in these complex tribosystems is studied on the basis of the theoretical concepts of irreversible thermodynamics. It is shown that a higher number of interrelated processes within the system result in an increased probability of self-organization. The results of this thermodynamic model are confirmed by the investigation of the wear performance of a novel $Ti_{0.2}Al_{0.55}Cr_{0.2}Si_{0.03}Y_{0.02}N/Ti_{0.25}Al_{0.65}Cr_{0.1}N$ (PVD) coating with complex nano-multilayered structure under extreme tribological conditions of dry high-speed end milling of hardened H13 tool steel.

Keywords: friction; entropy; non-equilibrium thermodynamics; composite materials

PACS Codes: 81.40.Pq; 05.70.Np; 05.70.Ln

---

1. Introduction

Adaptation of a cutting tool surfaces during friction is a process that is directly related to self-organization. In previous studies, it was shown that friction as a non-equilibrium process can be studied based on the concepts of non-equilibrium thermodynamics and self-organization. According to Klimontovich [1], self-organization is a process of dissipative structure formation that results in wear rate decrease within a tribosystem [2]. Fundamentally, dissipative structures occur in open systems and are part of non-equilibrium processes. These dissipative systems are characterized by their unstable nature. Thus there is significant motivation to establish a criteria to determine the likelihood of self organization occurring during friction. This is motivated by our goal to reduce wear. Classical irreversible thermodynamics and theory of self-organization to date, do not establish such a criteria.

There are several known systems in the world with dissipative structures where self-organization occurs. Well known examples of such systems are turbulent liquid motion, reaction of Belousov-Zabatinsky, chemical models of the "Brusselator" and "Oregonator". In tribology, an example of such a system is the beneficial lubricating action of tribofilms during machining [2]. If the tribosystem is acting in a stable pattern after initiating a self-organization process, then the self-organization is deemed a probabilistic process [3]. As was indicated prior, there is no criteria to determine if self-organization will occur, however there exists a condition to determine if self-organization has occurred. This condition is as follows: self-organization can begin only if the system has lost its thermodynamic stability.

Many modern tribological applications act under extreme conditions that can lead to catastrophic wear [4,5]. Dry ultra-high speed machining of hardened tool steels is a classical example of the extreme conditions. Under these conditions high temperatures and stresses [5] occur on the friction surface, followed by a number of simultaneously processes that result in complex frictional conditions [6]. In addition to intensive adhesion, rubbing, and tribochemical reactions on the contact surface due to interaction with the environment, there is also a high probability of thermal-fatigue for some operations [6,7].

Introduction of adaptive hard coatings [5] aims to tackle these issues. An idea of adaptive coatings came from understanding that any tribosystem combines some features of an artificial engineering system and a natural phenomenon (friction itself). Adaptability of a material is related to the changes in its characteristics in response to an external stimulus. Ideally these changes in material characteristics will lead to a diminishing effect of the stimulus [5]. This effect for example could be reduced friction which in turn will reduce wear. Adaptive coatings enable a tribosystem to shift to a milder wear mode instead of sustaining a severe wear mode [5]. Adaptation is directly related to self-organization phenomenon. This occurs with formation of dissipative structures (nanoscaled tribofilms) at the friction surface [5,8]. In tribological study of machine tools, these structures are generated from the structural modification of the hard coating by interaction with the environment [5].

One possible way to enhance adaptive properties is through the application of nanostructured coatings. Application of nanostructured coatings does not automatically result in the improvement of mechanical properties [5], but strongly affects their physicochemical properties [5]. Many modern materials synthesis techniques, including Physical Vapor Deposition (PVD) coatings deposition, take advantage of processes that occur far from thermodynamic equilibrium. PVD coatings result in a high

density of lattice imperfections [9]. This causes the creation of a surface with a highly non-equilibrium state and the potential to dramatically accelerate beneficial physicochemical reactions through formation of dissipative structures [2,5].

The Al-rich TiAlN family of nanostructured hard PVD coatings is widely used for high performance machining applications [5]. It was shown that this family of adaptive hard PVD coatings outperforms other categories of coatings in terms of wear rate under aggressive cutting conditions [4]. The systematic optimization of this Al-rich coating composition results in the occurrence and evolution of a synergistically alloyed TiAlCrSiYN-based coating [4]. However, it is a challenge to further improve this family of coatings.

The theoretical model presented is based on the consideration of self-organization during friction. In this study, complex wear resistant coatings that are nano-multilayered were compared against mono-layered coatings. A relation between complexity of the tribosystem (multilayered vs. mono-layered) and self-organization was investigated.

The goal of this study, is therefore to determine how the complexity of tribosystems affects the probability of attaining beneficial self-organization under aggressive machining conditions. This goal will be accomplished through the use of irreversible thermodynamics theory and will be validated *via* experimental data for various novel nano-multilayered hard coatings.

2. Theoretical Investigation

According to Prigogine [10–11], thermodynamic stability of a system is indicated by the sign of the second variation of entropy, S. If this value is negative, the system is inherently unstable. If a system is unstable equation (1) holds true [10–11]

$$\delta^2 S < 0 \tag{1}$$

Equation (1) is considered as Liapunov's function. Thus, the condition of stability is the following [10–11]:

$$\frac{\partial(\delta^2 S)}{\partial t} \geq 0 \tag{2}$$

In the same manner, the following equalities give the necessary condition of stability of the system:

$$\delta^2 S < 0 \text{ while } \frac{\partial(\delta^2 S)}{\partial t} \geq 0 \tag{3}$$

The second derivative of entropy with respect to time corresponds to entropy production. Entropy production in this case relates to a disturbance of the system to an external influence [11]. The following equation also holds true:

$$\frac{1}{2}\frac{\partial(\delta^2 S)}{\partial t} = \sum_n \delta X_n \delta J_n \geq 0 \tag{4}$$

where δX_n and δJ_n are deviations of the applicable fluxes and driving force, respectively in the stable state of the system. Examples of thermodynamic fluxes and forces are the following: heat flux and temperature gradient; gradient of chemical potentials and diffusion; difference in chemical affinity

and chemical reactions; gradient of mechanical stresses and deformation. All these processes are spontaneous and widely occur during friction.

The summation in equation (4) is known as the resulting entropy production. If at the occurrence of a disturbance, equality (4) is satisfied, then the state of the system is stable. However, for certain processes equation (4) can be negative. In this case, the state can become thermodynamically unstable. Only after passage through instability, the self-organization process can begin (see classical example of B**é**nard cell formation [3,11]). Therefore, a necessary condition for the self-organization process to occur is:

$$\frac{1}{2}\frac{\partial(\delta^2 S)}{\partial t} = \sum_n \delta X_n \delta J_n < 0 \tag{5}$$

Again, if equation (4) holds, then the system is in the stable state, while if equation (5) holds, then self-organization in the system is possible.

If there is only one process in the system which is non-linear and dissipative, then:

$$J_1 = L_1 X_1 \tag{6}$$

Here J_1 is the generalized flux, L_1 is the phenomenological coefficient and X_1 is the driving force. The subscript in this equation relates to how many processes are taking place in the system. The following relationship must also hold true. Equation (7) is the result of substituting equation (6)

$$\frac{d_i S}{dt} = \sum_k X_k J_k = \frac{J^2}{L} \tag{7}$$

The subscript *i*, in equation (7) is to characterize a specific thermodynamic process. The subscript k in equation (7) is mean to represent the thermodynamic variable of interest within the system such as coefficient of diffusion, chemical affinity *etc.*, that affect the system's response.

Next, assume that there exists parameter α that characterizes the degree of the system's deviation from equilibrium. For example in a nanostructured coating, α is the size of a nanostructural component [5]. The parameter α is related to the density of crystal structure imperfections within the coating layer. The quantity of imperfections in this case is increasing with reduction in size of the nanocomponent. These smaller size nano-crystals result in a higher value of parameter α [5].

The entropy production for this case is defined as follows:

$$\sum_k X_k J_k = \frac{1}{L}\left(\frac{\partial J}{\partial \alpha}\right)^2 (\delta\alpha)^2 \tag{8}$$

Equation (8) is a quadratic. For this system, when L > 0, the system cannot lose its stability. As proof of this result, according to equation (6), the coefficient L does not depend on parameter α,. This corresponds to the conclusion made by Gershman and Bushe [2] that the system cannot lose stability if only one process denoted by symbol i, is occurring.

Next we will assume that the coefficient L in (6) as it is shown in [18] depends on the parameter α. Then, the excessive entropy production is the following:

$$\sum_k \delta X_k \delta J_k = \left[\frac{1}{L}\left(\frac{\partial J}{\partial \alpha}\right)^2 - \frac{J}{L^2}\frac{\partial L}{\partial \alpha}\frac{\partial J}{\partial \alpha}\right](\delta\alpha)^2 \tag{9}$$

Excessive entropy production in equation (9) can be negative if the term $\frac{J}{L^2}\frac{\partial L}{\partial \alpha}\frac{\partial J}{\partial \alpha}$ is positive. To fulfill this requirement, the derivatives $\frac{\partial L}{\partial \alpha}$ and $\frac{\partial J}{\partial \alpha}$ must have the same sign, either positive or negative.

Let us consider the system, in which two non-linear and interrelated processes (two channels of dissipation) are occurring:

$$\begin{aligned} J_1 &= L_1 X_1 + L_{12} X_2 \\ J_2 &= L_2 X_2 + L_{21} X_1 \end{aligned} \tag{10}$$

The subscripts here (*i.e.* $L_{jk} = L_{12}$) characterize the interaction between the two irreversible processes. The entropy production for (10) will be as follows:

$$\frac{d_i S}{dt} = X_1 J_1 + X_2 J_2 = X_1 (L_1 X_1 + L_{12} X_2) + X_2 (L_2 X_2 + L_{21} X_1) \tag{11}$$

If we introduce parameter α in the same way it has been done in formula (9), then we get the following expression for entropy production:

$$\begin{aligned} \sum_k \delta X_k \delta J_k = [&\frac{\partial X_1}{\partial \alpha}\frac{\partial L_1}{\partial \alpha} X_1 + L_1 (\frac{\partial X_1}{\partial \alpha})^2 + \frac{\partial X_1}{\partial \alpha}\frac{\partial L_{12}}{\partial \alpha} X_2 + L_{12}\frac{\partial X_1}{\partial \alpha}\frac{\partial X_2}{\partial \alpha} + \frac{\partial X_2}{\partial \alpha}\frac{\partial L_2}{\partial \alpha} X_2 \\ &+ L_2 (\frac{\partial X_2}{\partial \alpha})^2 + \frac{\partial X_2}{\partial \alpha}\frac{\partial L_{21}}{\partial \alpha} X_1 + L_{21}\frac{\partial X_1}{\partial \alpha}\frac{\partial X_2}{\partial \alpha}](\delta\alpha)^2 \end{aligned} \tag{12}$$

Among the eight terms in the first brackets of the right part of equation (12), the six, non-squared terms can be negative.

For generalization, let us consider the system, in which three independent non-linear interrelated processes (three channels of dissipation) are occurring:

$$\begin{aligned} J_1 &= L_1 X_1 + L_{12} X_2 + L_{13} X_3 \\ J_2 &= L_2 X_2 + L_{21} X_1 + L_{23} X_3 \\ J_3 &= L_2 X_2 + L_{21} X_1 + L_{32} X_2 \end{aligned} \tag{13}$$

By introduction of parameter α, similarly to (9), we get the excessive entropy production:

$$\begin{aligned} \sum_k \delta X_k \delta J_k = [&\frac{\partial X_1}{\partial \alpha}\frac{\partial L_1}{\partial \alpha} X_1 + L_1 (\frac{\partial X_1}{\partial \alpha})^2 + \frac{\partial X_1}{\partial \alpha}\frac{\partial L_{12}}{\partial \alpha} X_2 + L_{12}\frac{\partial X_1}{\partial \alpha}\frac{\partial X_2}{\partial \alpha} + \frac{\partial X_1}{\partial \alpha}\frac{\partial L_{13}}{\partial \alpha} X_3 \\ &+ L_{13}\frac{\partial X_1}{\partial \alpha}\frac{\partial X_3}{\partial \alpha} + \frac{\partial X_2}{\partial \alpha}\frac{\partial L_2}{\partial \alpha} X_2 + L_2 (\frac{\partial X_2}{\partial \alpha})^2 \\ &+ \frac{\partial X_2}{\partial \alpha}\frac{\partial L_{21}}{\partial \alpha} X_1 + \frac{\partial X_2}{\partial \alpha}\frac{\partial X_1}{\partial \alpha} L_{21} + \frac{\partial X_2}{\partial \alpha}\frac{\partial L_{23}}{\partial \alpha} X_3 + L_{23}\frac{\partial X_2}{\partial \alpha}\frac{\partial X_3}{\partial \alpha} + \frac{\partial X_3}{\partial \alpha}\frac{\partial L_3}{\partial \alpha} X_3 \\ &+ L_3 (\frac{\partial X_3}{\partial \alpha})^2 + \frac{\partial X_3}{\partial \alpha}\frac{\partial L_{31}}{\partial \alpha} X_1 \\ &+ \frac{\partial X_3}{\partial \alpha}\frac{\partial X_1}{\partial \alpha} L_{31} + \frac{\partial X_3}{\partial \alpha}\frac{\partial L_{32}}{\partial \alpha} X_2 + \frac{\partial X_3}{\partial \alpha}\frac{\partial x_2}{\partial \alpha} L_{32}](\delta\alpha)^2 \end{aligned} \tag{14}$$

Among the eighteen terms in the first brackets of the right part of equation (14), fifteen terms can be negative. From (9), (12) and (14), we can make the following general conclusion. Therefore, in a system with one non-linear process (see equation (9)), one term can be negative. In the system with two non-linear processes (see equation (12)), six terms among eight terms can be negative. In the system with three non-linear processes (see equation (14)), fifteen terms among eighteen terms can be negative. Generalizing these statements, one can conclude that with a system with n non-linear processes consists of $2n^2$ terms, and $2n^2$- n of them could be negative. In all of these scenarios, if the sum of all terms is negative then the system loses thermodynamic stability.

Thus the probability of losing thermodynamic stability can be defined as the following relationship

$$\frac{2n^2 - n}{2n^2} = 1 - \frac{1}{2n} \tag{15}$$

From equation (15) one can therefore conclude that with the growth of interrelated processes, the probability of losing thermodynamic stability increases. As a direct result of this finding, the probability of self-organization grows as well. That means that the wear rate will reduce within the system.

The physical meaning of these considerations is the following. The higher the number of the interrelated processes within the system leads to the higher number of interactions between these processes and thus probability of the self-organization is growing. As it was outlined above, self-organization usually requires severe frictional conditions [4,5]. Under severe operating conditions wear rate grows. Once self-organization has started, the wear rate drops dramatically [2,5]. In more complex systems with higher amounts of the interacting processes, self-organization can start under the initial stages of friction (Figure 2, a-b). Therefore, the overall wear rate can be decreased.

Increasing the complexity of an engineered system must be controlled on the basis of the emergent properties of the system [4]. If the characteristics of the system are tuned in such a way that emergent properties enhance wear resistance, then the goal of control is achieved and functionality of the system is improved.

In our previous studies [4], we have shown that mono-layered nano-crystalline TiAlCrSiYN coatings present adaptive behavior under increasingly severe operating conditions. Self-organization during friction is associated with this phenomenon. An overall minimal entropy production occurs despite an intensifying external impact. This overall minimal growth in entropy is possible due to the counteractive effect of local entropy decrease due to self organization. In the current case, the beneficial mass transfer of coating elements such as Al, Cr or Si is initiated under heat generated during friction. This process, combined with interaction with the environment (tribo-oxidation) results in negative entropy production within the layer of tribofilms [4].

The tribosystem of dry end milling of hardened steels can also be analyzed to this effect. Such a system is a heavily loaded system that operates at high temperatures under permanent thermal-cycling impact, which leads to crack formation and propagation within the coating layers and eventually results in catastrophic surface damage. It is imperative we introduce a more complex design of the coating, in particular a nano-multilayered design. The novel coating consists of alternating layers with a modulating chemical composition but similar crystal structure. This coating has a hardness of 30 GPa. It is known that nano-multilayered coatings have the ability to dissipate energy with high

efficiency due to crack propagation along the nanolayer interfaces. This prevents surface damaging and reduces entropy production [12,13]. The successful use of such a coating could resist external impact during thermal cycling.

In this example, the number of interrelated processes is growing and the likelihood of self-organization in a complex tribosystem increases, resulting in wear rate reduction. This conclusion of the theoretical modeling is confirmed by the experimental data presented below.

3. Experimental

A nano-multilayered $Ti_{0.2}Al_{0.55}Cr_{0.2}Si_{0.03}Y_{0.02}N/Ti_{0.25}Al_{0.65}Cr_{0.1}N$ coating was deposited using $Ti_{0.2}Al_{0.55}Cr_{0.2}Si_{0.03}Y_{0.02}$ and $Ti_{0.25}Al_{0.65}Cr_{0.1}$ targets fabricated by powder metallurgical process on mirror polished cemented carbide WC-Co substrates and ball nose end mills in a R&D-type hybrid PVD coater (Kobe Steel Ltd.) using a plasma-enhanced arc source. Samples were heated up to approximately 500°C and cleaned through Ar ion etching process. Ar-N_2 mixture gas was fed to the chamber at a pressure of 2.7 Pa with a N_2 partial pressure of 1.3 Pa. The arc source was operated at 100 A for a 100 mm diameter x 16 mm thick target. Two targets were used for coating deposition. Other deposition parameters are as follows: bias voltage: 100 V; substrate rotation: 5 rpm. The thickness of the coating was around 3 microns for the film characterization and cutting test work. Coating thickness was measured by crater grinding methods using CALOTEST (CSM instruments). Typical accuracy of this measurement was around $\pm$ 0.1 mm. Cross-sectional TEM observation was employed in combination with FIB (focused ion beam) for investigation of the coatings on the cemented carbide WC/Co substrates. Transmission electron microscopy was performed in a JEOL FS2200 microscope at an acceleration voltage of 200 kV. The structural and phase transformations at the cutting tool/workpiece interface and the chemical composition of the tribofilms formed were studied by X-ray photoelectron spectroscopy (XPS) on a ESCALAB MK2 (VG) electron spectrometer equipped with a hemispherical energy analyzer. An X-ray tube with monochromatic Al K_α radiation ($h\nu$ = 1,486.6 eV) was used as an excitation source. A sector 0.5 x 5.0 mm was selected for surface analysis. The XPS signal was recorded in the mode CAE = 50.0 V at 0.25 eV/s.

The micro-mechanical characteristics of the coatings were measured on WC-Co using a Micro Materials NanoTest system. Nanoindentation was performed in load controlled mode with a Berkovich diamond indenter calibrated for load, displacement, frame compliance and indenter shape according to an ISO14577–4 procedure. The area function for the indenter was determined by indentations to 0.5–500 mN into a fused silica reference sample. For the nanoindentation into the coatings, the peak load was 40 mN and 40 indentations were performed for each coating. This load was chosen to minimize any influence of surface roughness on the data whilst ensuring that the indentation contact depth was under 1/10 film thickness so that a coating-only (load-invariant) hardness could be measured in combination with a coating-dominated elastic modulus. Nanoindentation was performed at room temperature. Nanoimpact testing was performed at room temperature with a NanoTest fitted with a cube corner indenter as an impact probe. The indenter was accelerated from 12 μm above the coating surface with 25 mN and 150 mN coil force to produce an impact every 4 s for a total test duration of 600s. The coatings' nanoimpact fatigue fracture resistance was assessed by the final measured impact depth and confirmed by microscopic analysis of impact craters. Micro-wear (low

cycling repetitive unidirectional sliding wear) tests were performed using the NanoTest Scratching Module with a 25 μm radius diamond probe. The 12-scan micro-wear procedure involved an initial topography scan followed by 10 scans where after a 200 μm leveling distance, the load was ramped quickly (100 mN/s) to the peak load of 0.5, 1 or 2 N, and then followed by a subsequent topography scan. The scan speed was 5 μm/s and the total scan length was 800 μm. On-load and post-load, probe penetration depth data in the constant load region (last 600 μm of each scan) were determined automatically after correction for the sample slope and frame compliance in the instrument software.

Oxidation resistance of the coating was studied by using Thermogravimetric –Analysis (TG) within a temperature range of 25–1,200°C in air. This range of temperatures was selected to mimic severe cutting conditions during high performance dry machining of hardened steels. Temperatures at the tool/chip interface can reach as high as 1,100°C [18]. To perform this test one side of the Pt foil (30 x 10mm 0.2mm thick) was coated with 3 μm multilayered coating and subjected to the TGA measurement. Uncoated Pt was used as a reference sample during the test to measure the relative weight gain of the multilayered coating. The weight ratio of the Pt foil to the coating was is around 1: 4.

Cutting tests were performed during dry ball-nose end milling of the hardened AISI H13 tool steel with hardness HRC 53–55 under agressive cutting conditions. Mitsubishi carbide end mills (D = 10 mm) 3 micron thick nano-multilayered $Ti_{0.2}Al_{0.55}Cr_{0.2}Si_{0.03}Y_{0.02}N/Ti_{0.25}Al_{0.65}Cr_{0.1}N$ coating were used. The cutting experiments were carried out on a three-axis vertical milling center (Matsuura FX-5). The cutting parameters were as follows: speed 300–700 m/min; feed: 0.06 mm/tooth; axial depth: 5.0 mm; radial depth: 0.6 mm was measured according to ISO 368 using an optical microscope (Mitutoyo model). The worn ball nose end mill tooling was fitted in a special holder in the microscope. The magnification of the microscope was 30x. Accuracy of measurement was within ± 5μm.

4. Results and Discussion

Figure 1. TEM images (FIB cross-sectional view) of the TiAlCrSiYN-based coatings: (a) mono-layered TiAlCrSiYN coating; (b) nano-multilayered TiAlCrSiYN/TiAlCrN.

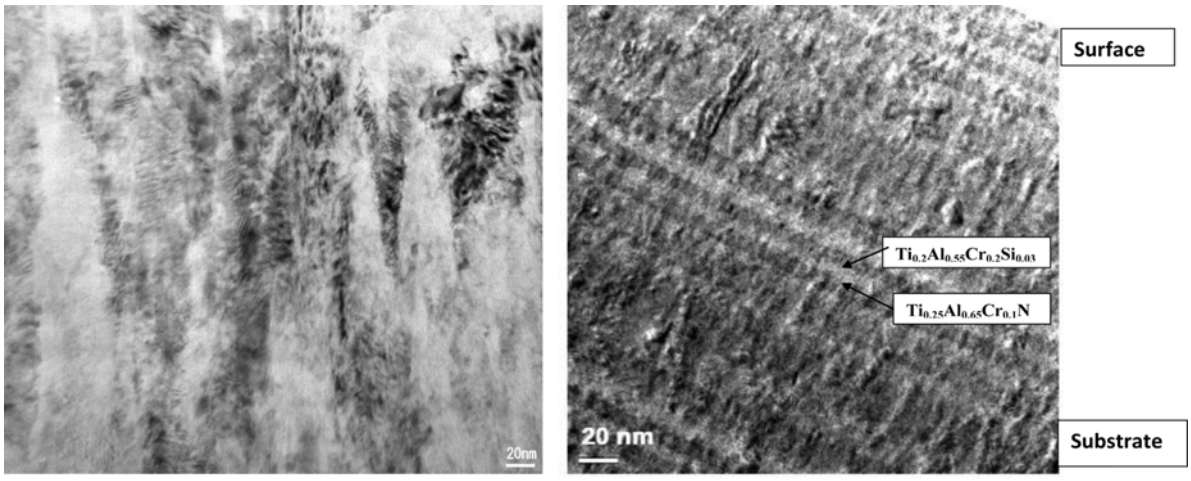

Figure 1 presents TEM images of a) the mono-layered $Ti_{0.2}Al_{0.55}Cr_{0.2}Si_{0.03}Y_{0.02}N$ coating and b) $Ti_{0.2}Al_{0.55}Cr_{0.2}Si_{0.03}Y_{0.02}N/Ti_{0.25}Al_{0.65}Cr_{0.1}N$ PVD nano-multilayered coatings. Both coatings mainly have B1 crystal structure. The columnar nano-grain structure is observed in the mono-layered coating (Figure 1, a) and the multi-layered coating (Figure 1, b) that combines nano-multilayered structure with modulating $Ti_{0.2}Al_{0.55}Cr_{0.2}Si_{0.03}Y_{0.02}N/Ti_{0.25}Al_{0.65}Cr_{0.1}N$ composition and columnar structure (Figure 1, b). The continuous columnar growth was thought to be possible as the alternating layers have the same B 1 crystal structure.

This complex nano-multilayered coating structure results in improvement of some micro-mechanical properties and promotes beneficial tribo-chemical reactions on the friction surface. The major properties of the coating are shown in Table 1.

Table 1. Properties of TiAlCrSiYN-based coatings.

Coating	Structure of the coatings		Properties of the coatings				
	Category of the coating	Crystal structure	Micro-hardness, GPa	Maximal impact depth, nm at impact forces		Low cycling wear test data, force of 2N	Weight gain, TG (%) after short-term (0.5 hr) oxidation in air at 1,100°C
				25 mN	150 mN		
TiAl55CrSiYN	Nano-crystalline Mono-layered	B1	29.9	2009	6155	Adhesion failure (after 3 cycles)	0.026
TiAl55CrSiYN / TiAlCrN	Nano-crystalline Nano-multilayered	Alternating layers with B1 structure; Minor amount of AlN hex phase	31.7	1791	5900	Gradual wear	0.010

To illustrate controlled improvement in the properties the novel nano-multilayered coating is compared to the prior mono-layered $Ti_{0.2}Al_{0.55}Cr_{0.2}Si_{0.03}Y_{0.02}N$ coating [4]. Hardness of the mono- and multilayered coatings was similar. Impact fatigue fracture resistance is slightly better for the multi-layered coating (Table 1). Low cycling scratch wear test data reveals differences in deformation behaviour (Table 1). Under forces of 2N (when the stress field reaches the interface) the mechanism on the multi-layered coating is a gradual failure. The mono-layered coating after initially showing lower wear, presented increased damage due to adhesion failure (cycle 3, Table 1). The improved fatigue related properties of the multilayered coating will control wear behavior of the coatings considerably.

Thermogravimetric (TG) data (Table 1) indicates a very low weight gain of the multilayered coating under the operating temperatures in air (0.01% against already low 0.03% for the mono-layered coating at 1,100 °C).

Figure 2, shows wear resistance data for the multilayered coatings compared to the mono-layered coating at speeds of 500 m/min [6]. The multilayered coating outperforms the mono-layered coating.

Stabilization of the wear rate for the multilayered coating takes place within the initial cutting stages: after a length of cut of 20 m a stable wear stage begins (see insert in Figure 2, a). The catastrophic wear begins after 250 m of cutting. Figure 2, b shows tool life of cutting tools of the multi-layered coating at a cutting speed of 600 m/min. The useful tool life in this case was approximately 100 m. Moreover, in spite of cutting speed growth, stabilization of the wear rate for the multi-layered coating takes place during the initial stages of cutting. The stable wear stage lasts up to 85 m, which is very long given the extreme conditions.

Cracks develop in the mono-layered coating layer due to friction and thermal-mechanical shock absorption. This eventually results in tool failure at the cutting edge. Based on the impact fatigue fracture resistance and low cycling scratch wear test data (Table 1), we can conclude that in the nano-multilayered coatings, the cracks can be deflected by the internal interfaces of the nano-layers, which results in energy dissipation without coating failure [12,13].

Figure 2. Comparative tool life of cutting tools with novel multi-layered TiAl55CrSiYN/TiAlCrN coating with prior state of art mono-layered TiAl55CrSiYN coating at varying cutting speeds during dry machining of hardened steels: (a) comparison 500 m/min; (b) 600 m/min; Initial stages of wear are shown in details in the insert.

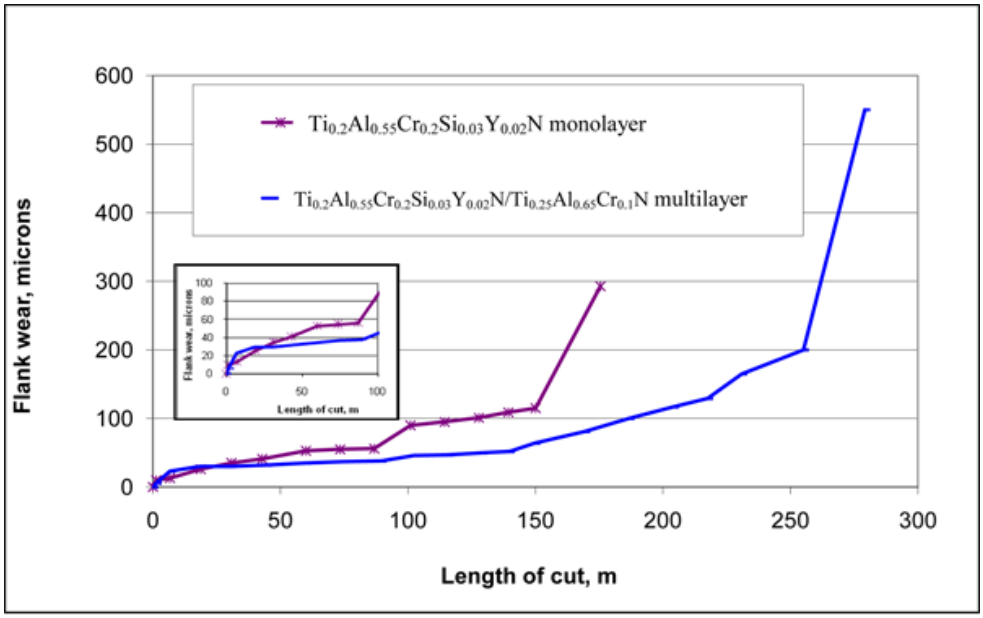

(a)

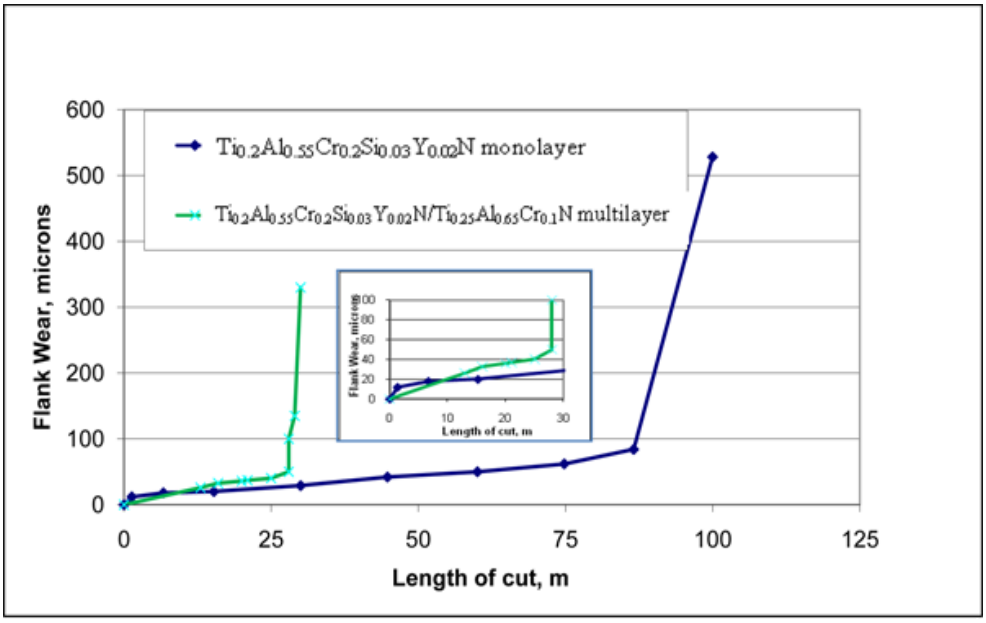

(b)

To study characteristics of the tribofilms, X-ray Photoelectron Spectroscopy (XPS) analysis of the worn tool surface was made (Table 2). A significant amount (around 15.9%) of lubricating [14] chromium oxides were generated (Table 2). A partial chemical transformation of aluminum in the multi-layered coating is taking place: 19.3% of Al retains in the complex nitride, 6.6% of aluminum oxidizes with formation of complex Al-Si-O oxide (mullite), 29.1% aluminum oxides with the formation of Al_2O_3 (sapphire) [16], which is twice the value compared to mono-layered coating (Table 2). The non-stoichiometric titanium tribo-oxide (7.3%) and rutile TiO_2 (5.5%, Figure 4, c) are forming on the friction surface as well. Small amounts of non-equilibrium SiOx phase were present on the friction surface as well. The phase composition of tribo-oxides differs for these two coatings: considerably higher concentration of Al_2O_3 is formed during tribooxidation of the multilayered coating.

Table 2. Phase and chemical composition of theworn surface.

Coating	Chemical elements content in the coating and tribo-films							
	Al, at%			Ti, at%			Cr, at%	
	Al_2O_3 tribo-film	Mullite tribo-film	Nitride coating	TiO_x tribo-film	TiO_2 tribo-film	Nitride coating	Cr_xO_y tribo-film	Nitride coating
multilayer	29.1	6.6	19.3	7.3	5.5	7.2	15.9	4.1
monolayer	8.8	17.6	28.6	6.8	7.2	6.0	16.0	4.0

Formation of a wide variety of refractory compound tribo-films led to excellent protection as well as lubrication of the surface under increasingly severe frictional conditions (Figure 2, b). The sapphires and mullites are known as hard oxide crystals that possess high strength, and excellent thermal shock resistance at high temperatures [16,17]. Chromium and silicon oxides have lubricating properties at

high temperatures [14,15]. This shifts the friction to a milder mode [5], reducing wear rate. Therefore formation of the protective and lubricious tribofilms is a desirable way for the tribo-system to adapt to the extreme frictional conditions.

To fully understand the cause of improvement in wear performance of the multi-layered coating we have to consider combination of all characteristics of the coatings. Tuned characteristics in complex engineering systems work as a whole. The ability of the system to adapt to the changing external environment is strongly enhanced if this synergistic effect exists. Simply put, the greater the number of simultaneous processes occurring in a tribosystem, the greater the chance that self-organization will occur.

Critical features of the coating acting in synergy will now be discussed. Initially, friction heats the surface. In response, this initiates a beneficial mass transfer of the coating's elements (Al, Cr, Si) to the friction surface. The nanostructured coating possesses an improved mobility and reactivity of the elements to transport them to the friction surface. This is followed by a beneficial tribo-oxidation due to interaction with the environment leading to the formation of dynamically stable tribofilms. This is related to the self-organization phenomenon. Minimal entropy production despite an intensifying external impact results due to this reaction [4]. The stability of minimal entropy production is provided by the complex interaction of different processes. Growth in entropy production caused by one of the processes- friction under increasingly severe conditions - is compensated by the reduction in entropy reduction in another process (beneficial mass transfer with further tribo-oxidation).

Another important feature of the coating is its nano-multilayered structure, which is able to efficiently dissipate thermo-mechanical energy supplied to the friction surface. This reduces intensity of the surface damaging process, which otherwise will cause a significant wear rate [13]. The multi-layered coating with its improved ability to dissipate energy of friction due to increased fatigue properties (Table 1) stays stable on the friction surface thus providing a protective/lubricating function (Figure 2, a-b). As a result, the wear rate stabilizes rapidly and stays stable for a prolonged period of time (see inserts in Figure 2, a-b).

In these systems one particular characteristic (*i.e.* micro-mechanical, Table 1) can affect other categories of characteristics (*i.e.* stable regeneration of protective/lubricious tribo-films, Table 2) and vice versa. As a result, the characteristics are integrated within the system and work in synergy. This is typical of systems with dissipative structures and an emergent behavior. A tribosystem with this behavior can accumulate more energy without significant surface damage and wear rate increase. It is worth noting that the emergent behavior of the coating can be assessed though various properties of the coating shown in Table 1. It is thus important when tuning a coating to improve a particular property but not cause a critical decrease in performance of another property. If this procedure is followed, an adaptive coating with emergent properties is able to sustain severe operating conditions and increase tool life under aggressive cutting conditions.

5. Conclusions

It was shown based on the concept of irreversible thermodynamic that increasing tribo-system complexity increases the probability of self-organization. During friction this self-organization leads to wear rate reduction.

The trends outlined in this theoretical model were confirmed by investigation of the wear performance of a complex surface engineered tribosystem. This complex surface engineered coating was a nano-multilayered $Ti_{0.2}Al_{0.55}Cr_{0.2}Si_{0.03}Y_{0.02}N/Ti_{0.25}Al_{0.65}Cr_{0.1}N$ wear resistant PVD coating. It consisted of alternating layers with modulating chemical composition, but similar crystal structure and hardness. The coating was a complex multilayered structure with nano-grain intergrowth within the alternating nano-layers. This coating had a number of tuned characteristics, such as improved micro-mechanical properties and high oxidation stability which were integrated in a way to work in synergy. As a result, the coating was able to stay on the frictional surface for a longer duration of time, while simultaneously being capable of enhancing dynamic regeneration of the tribofilms (dissipative structures) that were formed as a result of the self-organization process. This resulted in a tool surface which efficiently protected and lubricated to adapt to extreme tribological conditions. As a result, tool life was prolonged.

References and Notes

1. Klymontovich, Yu. L. *Introduction to the physics of open systems*; Yanus-K: Moscow, Russia, 2002.
2. Gershman, I.S.; Bushe, N.A. Elements of Thermodynamics and Self-Organization during Friction. In *Self-Organization during Friction. Advanced Surface-Engineered Materials and Systems Design*; Fox-Rabinovich, G.S., Totten, G.E., Eds.; CRC Taylor & Francis: Boca Raton, FL, USA, 2006.
3. Nicolis, G.; Prigogine, I. *Self-Organization in Nonequilibrium Systems*; John Wiley & Sons: New York, NY, USA, 1977.
4. Fox-Rabinovich, G.S.; Veldhuis, S.C.; Dosbaeva, G.K.; Yamamoto, K.; Gershman, I.S.; Kovalev, A.; Beake, B.D.; Shuster, L.S. Nano-crystalline coating design for extreme applications based on the concept of complex adaptive behavior. *J. Appl. Phys.* **2008**, *103*, 083510.
5. Fox-Rabinovich, G.S.; Totten G., Eds. *Self-organization during friction: Advance Surface Engineered Materials and Systems Design*; CRC Taylor and Francis Group: Boca Raton, FL, USA, 2006.
6. Löffler, F.H.W Systematic approach to improve the performance of PVD coatings for tool applications. *Surface Coating Technol.* **1994**, *68–69*, 729–740.
7. Trent, E. M.; Wright, P.K. In *Metal Cutting*, 4th ed.; Butterworth-Heinemann: Boston, MA, USA, 2000.
8. Prigogine, I. *From Being to Becoming*; WH Freeman and Company: San Francisco, CA, USA, 1980.
9. Palatnik, L.S. *Pores in the Films*; Energoizdat: Moscow, Russia, 1982.
10. Prigogine, I.; Stengers, I. *Order Out of Chaos*; Bantam: New York, NY, USA, 1984.
11. Glansdorff, P.; Prigogine, I. *Thermodynamic theory of structure, stability and fluctuation*; Wiley–Interscience: London, England, 1970.

12. Karimi, A.; Wang, Y.; Cselle, T.; Morstein, M. Fracture mechanisms in nanoscale layered hard thin films. *Thin Solid Film.* **2002**, *275*, 420–421.
13. Shevela, V.V. Peaks of tool life during metal cutting. *Trenie. I. Iznos*. *(Russian J. Friction and Wear*) **1990**, *11*, 136–142.
14. Fox-Rabinovich, G.S.; Yamomoto, K.; Veldhuis, S.C.; Kovalev, A.I.; Dosbaeva, G.K. Tribological Adaptability of TiAlCrN PVD Coatings under High Performance Dry Machining Conditions. *Surface Coating. Technol.* **2005**, *200*, 1804–1813.
15. Honda, F.; Saito, T. Tribochemical characterization of the lubrication film at the Si_3N_4/Si_3N_4 interface sliding in aqueous solutions. *Appl. Surf. Sci.* **1992**, *92*, 651–655.
16. Yates, J.T. Surface chemistry of silicon - the behaviour of dangling bonds. *J. Phys.: Condens. Matter* **1991,** *3*, S143-S153.
17. Lanin, A.G.; Muravin, E.L.; Popov, V.P.; Turchin, V.N. Thermal shock resistance and thermal-mechanical processing of sapphire*, J. Eur. Ceram. Soc.* **2003,** *23*, 455.
18. Jou. D.; Casas-Vazques, J.; Lebon, G. *Extended Irreversible Thermodynamics*; Springer-Verlag: Berlin-Heidelberg, Germany, 2001.